



HAL
open science

Thermodynamic characterization of mixed gas hydrates in the presence of cyclopentane as guest molecule for an application in secondary refrigeration

Nada Chami, Sabrina Bendjenni, Didier Dalmazzone, Pascal Clain, Véronique Osswald, Anthony Delahaye, Laurence Fournaison

► To cite this version:

Nada Chami, Sabrina Bendjenni, Didier Dalmazzone, Pascal Clain, Véronique Osswald, et al.. Thermodynamic characterization of mixed gas hydrates in the presence of cyclopentane as guest molecule for an application in secondary refrigeration. *Chemical Engineering Science*, 2021, 244, pp.116790. 10.1016/j.ces.2021.116790 . hal-03252054

HAL Id: hal-03252054

<https://ensta-paris.hal.science/hal-03252054>

Submitted on 13 Jun 2023

HAL is a multi-disciplinary open access archive for the deposit and dissemination of scientific research documents, whether they are published or not. The documents may come from teaching and research institutions in France or abroad, or from public or private research centers.

L'archive ouverte pluridisciplinaire **HAL**, est destinée au dépôt et à la diffusion de documents scientifiques de niveau recherche, publiés ou non, émanant des établissements d'enseignement et de recherche français ou étrangers, des laboratoires publics ou privés.



Distributed under a Creative Commons Attribution - NonCommercial 4.0 International License

Thermodynamic characterization of mixed gas hydrates in the presence of cyclopentane as guest molecule for an application in secondary refrigeration.

Nada CHAMI^{1,2}, Sabrina BENDJENNI¹, Pascal CLAIN^{3,2}, Véronique OSSWALD², Anthony DELAHAYE², Laurence FOURNAISON², Didier DALMAZZONE^{1*}.

1 UCP/ENSTA Paris, Institut Polytechnique de Paris, Palaiseau, France

2 Université Paris-Saclay, INRAE, FRISE, 92761, Antony, France

3 Léonard de Vinci Pôle Universitaire, Research Center, 92916 Paris la Défense, France

* Corresponding author didier.dalmazzone@ensta-paris.fr

Abstract

Gas hydrates have drawn the attention of many scientists because of their potential role in energy applications. By using some thermodynamic promoters, it is possible to form hydrates at reduced pressure and near ambient temperature, which are suitable formation conditions for most industries. In this study, a high pressure micro differential scanning calorimeter was used to measure the dissociation conditions of mixed cyclopentane (c-C₅H₁₀) + CO₂ hydrates in the system composed of liquid water + liquid hydrocarbon + hydrate + vapour, in a pressure range of 0 to 4.3 MPa in a temperature range of 280 to 292 K. The analysis of the heat flow curve allowed the direct determination of the dissociation enthalpy of c-C₅H₁₀ + CO₂ hydrates (e.g., $\Delta H = 462.5 \pm 1.5$ kJ. kg⁻¹ water at equilibrium pressure 0.25 MPa) and the average mass heat capacity of c-C₅H₁₀ + CO₂ hydrates in a temperature range of [277.9 – 281.2] K ($C_{pH} = 1479.09 \pm 137.43$ J. K⁻¹. kg⁻¹ hydrate at 0.25 MPa).

Keywords: DSC, gas hydrates, cyclopentane, phase equilibrium, composition, dissociation enthalpy, mass heat capacity.

Abbreviations

P	Pressure
T	Temperature
\dot{q}	Heat flow
Z	Gas compressibility
R	Universal gas constant
ΔH_1	Enthalpy of dissociation per mole of carbon dioxide calculate from Clausius-Clapeyron method
ΔH_2	Enthalpy of dissociation per mole of water measured with the DSC method
C_{p1}	Mass heat capacity in the system before dissociation
C_{p2}	Mass heat capacity in the system after dissociation
C_{pH}	c-C ₅ H ₁₀ + CO ₂ hydrate mass heat capacity in the system before dissociation
$C_{p-c-C_5H_{10}}$	Mass heat capacity of cyclopentane
m_H	Hydrate formed mass
$m_{c-C_5H_{10}}$	Mass of cyclopentane in the system before dissociation of c-C ₅ H ₁₀ + CO ₂ hydrate
$m'_{c-C_5H_{10}}$	Mass of cyclopentane in the system after dissociation of c-C ₅ H ₁₀ + CO ₂ hydrate
m_{H_2O}	Mass of water in the system before dissociation of c-C ₅ H ₁₀ + CO ₂ hydrate
m'_{H_2O}	Mass of water in the system after dissociation of c-C ₅ H ₁₀ + CO ₂ hydrate
m_{CO_2}	Mass of carbon dioxide in the system before dissociation of c-C ₅ H ₁₀ + CO ₂ hydrate
m'_{CO_2}	Mass of carbon dioxide in the system after dissociation of c-C ₅ H ₁₀ + CO ₂ hydrate

1. Introduction

Gas hydrates are crystalline structures belonging to the family of clathrates (from "klathron" in Greek, which means closure). These are inclusion compounds that form a network of water molecules called hosts, which are filled by another so-called guest/invited/included molecule. Three different structures are usually formed for gas hydrates: structure I (sI), structure II (sII), and structure H (sH) determined by the size of the guest molecules (Jeffrey, 1984).

The thermodynamic stability and thermophysical properties of clathrate hydrates depend on hydrate structure, the trapped molecular species, but also on the cage occupancy for each invited molecule. Many experimental measurements of thermophysical properties are required to obtain a complete data set, including the phase diagram, composition of gas hydrates at variable pressure, dissociation enthalpy, and heat capacity (Carroll, 2014). Various studies have been conducted on hydrate-liquid-vapour-equilibrium data for several applications, such as gas separation (Mondal *et al.*, 2012), gas transport (Taheri *et al.*, 2014), and refrigeration (Marinhas *et al.*, 2006; Oyama *et al.*, 2005; Wenji *et al.*, 2009)

The complete determination of thermophysical properties, particularly useful in the field of refrigeration, is rare. The use of gas hydrates as phase-change materials (PCM) for secondary refrigeration using two phases fluid (hydrate slurries), is an alternative solution to reduce greenhouse gas emission of refrigerant as HFCs. CO₂ hydrates have been identified as a good PCM candidate in secondary refrigeration (Oignet *et al.*, 2017) because of their advantage of being formed by a non-mechanical process of gas injection into a cooled liquid phase (compared to ice slurries) and also because of their high dissociation enthalpy (Marinhas *et al.*, 2006).

The use of CO₂ hydrate in cold transport has been investigated. Therefore, these hydrates must have a high energy density to be used.

However, the formation of CO₂ hydrates at high pressure and low temperature hinders the industrial development of these processes (Clain *et al.*, 2015; Kang and Lee, 2000). Therefore, some studies have shown that the use of additives can reduce the equilibrium pressure. Many investigations on gas hydrate equilibrium conditions in systems containing water + CO₂ + additive, including tetrahydrofuran (THF), cyclopentane, cyclohexane, methyl cyclopentane (Mohammadi and Richon, 2009), and quaternary ammonium salts (Mayoufi *et al.*, 2010; Sakamoto *et al.*, 2011) have been carried out and have shown a significant reduction in pressure formation..

Table 1 shows the experimental conditions studied in the literature for carbon dioxide and cyclopentane as promoter. (Mohammadi and Richon, 2009) have detailed the hydrate equilibrium conditions for CO₂ hydrate systems with methyl cyclopentane, methyl cyclohexane, and cyclopentane. The comparison of experimental hydrate equilibrium data reported in the literature leads to the conclusion that cyclopentane is the most effective among all the promoters used.

(Zhang and Lee, 2009) presented experimental results of the formation/ dissociation conditions for carbon dioxide hydrates with cyclopentane compared to THF and TBAB. They showed that the dissociation temperature of mixed *c*-C₅H₁₀ + CO₂ hydrates at the same pressure was slightly higher than that with the other two other additives; (Matsumoto *et al.*, 2014) also presented the thermodynamic equilibrium data of gas hydrates with cyclopentane and its derivatives over a large range of pressure [0.08 – 4.88] MPa and temperature [274.2 – 293.7] K. They showed that the maximum dissociation temperature is reached at a pressure around 3 MPa and determined the dissociation enthalpy of mixed *c*-C₅H₁₀ + CO₂ hydrates at 308 ± 29 kJ.mol⁻¹ of hydrates using

Clausius-Clapeyron equation; then. (Herslund *et al.*, 2014) performed an experimental study on the dissociation of CO₂ hydrates dissociation with cyclopentane in a 5 mol % THF, which reduced the hydrate formation pressure by 20 % compared to the cyclopentane promoted system at a similar temperature.

Finally, (Lee *et al.*, 2019) investigated the mixed c-C₅H₁₀ + CO₂ hydrates formation using differential scanning calorimetry (DSC) over a temperature range [285.1 – 292.2] K and pressure [0.60 – 3.78] MPa. The obtained enthalpy of dissociation ΔH was equal to $491.4 \pm 7.4 \text{ J.g}^{-1}$ water and a hydration number of 7.6 was found at 3 MPa.

Table 1: Experimental condition results of c-C₅H₁₀+CO₂ hydrates in the literature

Author	Method	Temperature (K)	Pressure (MPa)	ΔH_d
(Zhang and Lee, 2009)	Micro DSCVII	[286.6 – 292.6]	[0.89 – 3.51]	-
(Mohammadi and Richon, 2009)	Isochoric pressure	[284.3 – 291.8]	[0.35 – 2.52]	-
(Herslund <i>et al.</i> , 2014)	Isochoric temperature	[280.1 – 291.6]	[0.08 – 4.88]	-
(Matsumoto <i>et al.</i> , 2014)	Clapeyron equation	[285.1 – 292.2]	[0.60 – 0.96]	$308 \pm 29 \text{ kJ.mol}^{-1}$ of hydrates
(Lee <i>et al.</i> , 2019)	HP μ DSC	[285.1 – 292.2]	[0.60 – 3.78]	$491.4 \pm 7.4 \text{ J.g}^{-1}$ of water

In the present work, the dissociation temperatures of c-C₅H₁₀ + CO₂ hydrates in a pressure range of [0.1 - 4.3] MPa are presented. The dissociation enthalpies of the c-C₅H₁₀ + CO₂ mixed hydrates were determined directly by the MicroDSC and estimated using the Clausius-Clapeyron equation. The experimental results are compared with the literature. The second part of this work is devoted to the determination of the composition of mixed c-C₅H₁₀ + CO₂ hydrates and the measurement of their mass heat capacity. One of the originalities of the present work is the determination of the dissociation enthalpy and the hydration number of c-C₅H₁₀ + CO₂ mixed hydrates at different pressure and temperature conditions. The determination of the specific heat capacity of mixed c-C₅H₁₀ + CO₂ hydrate is another originality presented by the paper presents.

2. Materials and methods

2.1 Materials

The experiments were carried out with distilled water. Cyclopentane was purchased from Sigma Aldrich (Molar purity: 0.98), carbon dioxide was obtained from Air Liquide (Molar purity: 0.99995). All materials were used without further purification.

2.2 Equipments

Figure 1 is a schematic representation of the main experimental setup for measuring hydrate dissociation temperatures in a high-pressure Micro DSC VII (SETARAM). A Differential Scanning Calorimetry (DSC) can identify transformations that affect heat flow, namely phase changes or endothermic or exothermic chemical reactions. It has long been used to study phase change thermodynamics, and to measure the thermophysical properties of phase change materials used in cold storage and transfer in refrigeration applications. In the present configuration, the DSC is equipped with gas-tight cells capable of withstanding pressures up to 40 MPa. A pressure sensor is connected to the DSC data logger to record pressure changes during the temperature program.

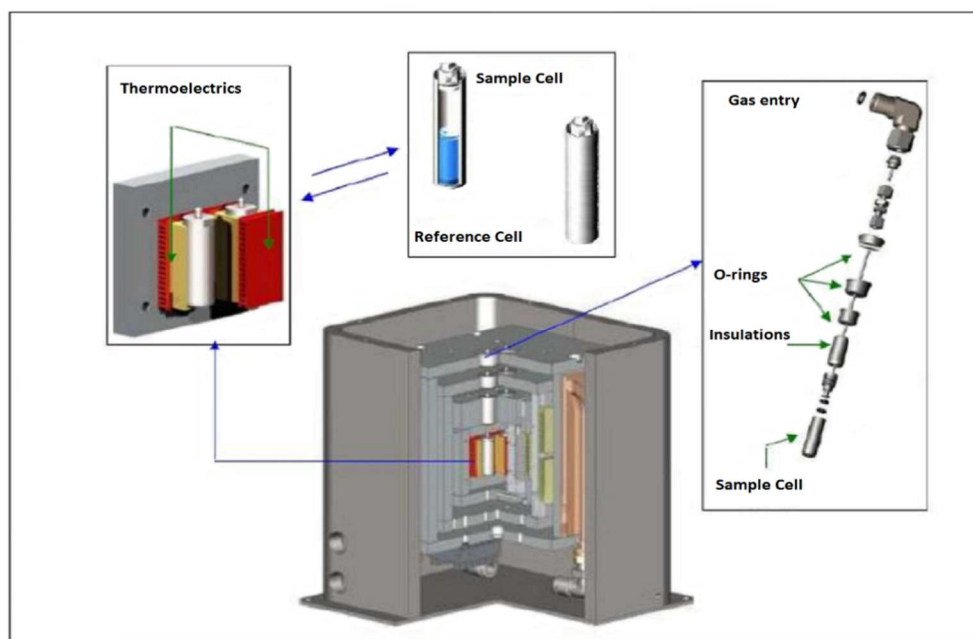


Figure 1: Representation of the main experimental setup in a Micro DSCVII (SETARAM).

There are two identical cells, one containing the sample and the other serving as a reference. The sample cell was filled with 0.05 cm^3 of distilled water and 0.1 cm^3 of $c\text{-C}_5\text{H}_{10}$, then CO_2 gas was injected. The temperature range varied from 253.1 K to 281.1 K and the CO_2 pressure range was up to 4.0 MPa.

2.3 Methods

The aim of the experiments was to determine p - T equilibrium points of the hydrates aqueous liquid-organic liquid-vapour ($\text{H-L}_W\text{-L}_{c\text{-C}_5\text{H}_{10}}\text{-V}$), the hydrates dissociation enthalpies, the heat capacity and the approximate composition in the systems $c\text{-C}_5\text{H}_{10} + \text{CO}_2 + \text{H}_2\text{O}$ at different CO_2 pressures. An excess of $c\text{-C}_5\text{H}_{10}$ (mass ratio of water to 1:2) was used in all experiments. The experimental procedure for the measurements of mixed $c\text{-C}_5\text{H}_{10} + \text{CO}_2$ hydrates formation parameters in water is as follows:

First, the liquid samples (50 μl of water and 100 μl of cyclopentane) were introduced into the DSC cell and weighed using a precision analytical balance (resolution $\pm 0.01\text{mg}$). Due to the very poor miscibility of $c\text{-C}_5\text{H}_{10}$ and water, the two liquids remained separated, with a water droplet at the bottom of the cell surrounded by an excess of cyclopentane. The cell was placed in a calorimeter block that was continuously purged with a stream of nitrogen to avoid water condensation during the cooling phases. The cell was then connected to the CO_2 supply line and purged at least five times to evacuate the remaining air. The initial pressure of CO_2 was set to the desired value. It should be noted that the set pressure corresponds to the initial conditions. The pressure in the cell would then depend on the gas dissolution in the liquids, the gas consumption during hydrate formation or the release of the hydrate during dissociation. The pressure would depend on the temperature program imposed on the cell. By recording the pressure signal along with the usual temperature and heat flow signals, it is possible to accurately track the gas pressure variation within the cell throughout the program. As mentioned by Martinez et al. (Martinez Valentin-Gamazo, 2009), various solids can occur in the ternary system $c\text{-C}_5\text{H}_{10} + \text{CO}_2 + \text{water}$ mixture:

single hydrates ($c\text{-C}_5\text{H}_{10}$ and/or CO_2 hydrates), mixed $c\text{-C}_5\text{H}_{10} + \text{CO}_2$ hydrates, and ice. A competition between the different kinds of hydrates took place between ice and $c\text{-C}_5\text{H}_{10}$ hydrates and more stable $c\text{-C}_5\text{H}_{10} + \text{CO}_2$ hydrates. To maximize the conversion rate of the $c\text{-C}_5\text{H}_{10}\text{-CO}_2\text{-H}_2\text{O}$ mixture to $c\text{-C}_5\text{H}_{10} + \text{CO}_2$ hydrates, a sequence of cooling and warming cycles was applied to successively crystallize and melt metastable phases (ice and single cyclopentane hydrate) and accumulate the stable mixed hydrate. For this purpose, the upper temperature of the cycles was set to values that do not reach the dissociation temperature of mixed hydrates (here warming temperature was 281.15 K). Figure 2 shows the heat flow and pressure evolutions during a typical cycling sequence realized to obtain the mixed $c\text{-C}_5\text{H}_{10} + \text{CO}_2$ hydrates. This run was performed at a CO_2 pressure of 0.25 MPa. During each thermal cycle, we observed that the crystallization and dissociation peaks decreased, indicating the disappearance of the less stable solids in the system. When both peaks are stable and no further evolution is observed a slower heating program is applied to achieve complete dissociation of the mixed $c\text{-C}_5\text{H}_{10} + \text{CO}_2$ hydrates.

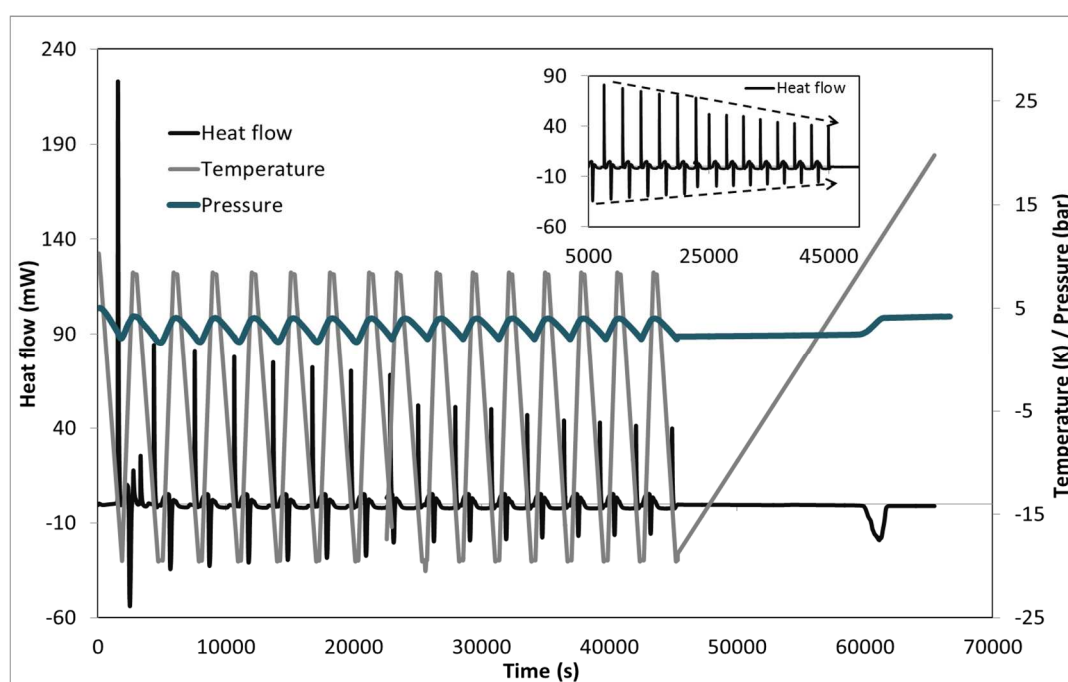


Figure 2: Thermal cycles for $c\text{-C}_5\text{H}_{10} + \text{CO}_2$ hydrates at 0.25 MPa to improve the conversion of $c\text{-C}_5\text{H}_{10}\text{-H}_2\text{O}\text{-CO}_2$ solution to $c\text{-C}_5\text{H}_{10} + \text{CO}_2$ hydrates

3. Results and discussion

This part focuses on the results related to the dissociation of mixed $c\text{-C}_5\text{H}_{10} + \text{CO}_2$ hydrate in the MicroDSC. For all experiments, the initial volume of water and cyclopentane is the same. First, the experimental dissociation data for $c\text{-C}_5\text{H}_{10} + \text{CO}_2$ hydrates are reported at different pressures and temperatures and compared with the literature data (Section 3.1). The dissociation enthalpy of $c\text{-C}_5\text{H}_{10} + \text{CO}_2$ is determined by two different methods: Clausius-Clapeyron equation and the heat flow integration (Section 3.2). Then, the composition of the mixed hydrates is presented based on the dissociation enthalpy results (Section 3.3). Finally, the dissociation thermogram at an initial pressure of 0.275 MPa (which corresponds to an equilibrium pressure of 0.25 MPa) is used to calculate the heat capacity of $c\text{-C}_5\text{H}_{10} + \text{CO}_2$ hydrates. The equilibrium point at (0.25 MPa, 282.4 K) was chosen because it provided a better dissociation peak which allowed the determination of the mass heat capacity (Section 3.4).

3.1 $L_w-L_c-C_5H_{10}-H-V$ equilibrium points

An extract from the DSC thermogram of the heating sequence after hydrates formation is shown in Figure 3. It must be remembered that only dissociation experiments are used for equilibrium determinations, since crystallization of aqueous phases, especially hydrates, is subject to large subcooling. As this type of DSC experiment is dynamic, the system can only be considered close enough to equilibrium when the heat flow is close to zero, which corresponds to the onset point of the dissociation peak as shown in Figure 3. The P_{onset} point corresponds to the first inflection point of the pressure signal. A perpendicular projection of the inflection point of the heat flow signal gives the onset temperature T_{onset} . It is noticeable that the onset temperature coincides exactly with the onset of the pressure signal. This indicates that the gas is released at the same time that heat starts is consumed to ensure hydrate dissociation. Thus, the coordinates of the equilibrium point are $(T_{\text{onset}}, p_{\text{onset}})$.

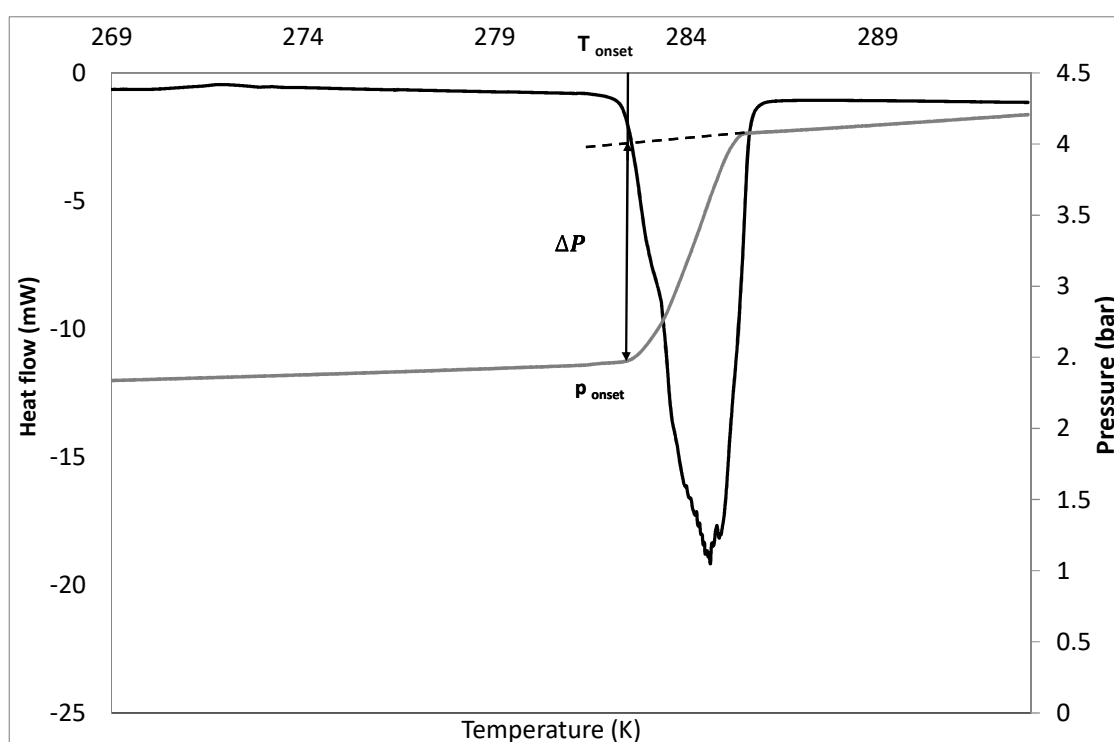


Figure 3: Typical dissociation thermogram of mixed $c-C_5H_{10} + CO_2$ hydrates under a pressure of 0.25 MPa of CO_2

The dissociation temperatures of mixed $c-C_5H_{10} + CO_2$ hydrates at equilibrium pressures ranging from [0.1 - 4.3] MPa are listed in Table 2. These results are plotted in Figure 4 and compared to those published in the literature.

Table 2: Dissociation temperature of mixed c-C₅H₁₀ + CO₂ hydrates at different pressures obtained by Micro DSC

T /K (± 0.2 K)	p /MPa	T /K (± 0.2 K)	p /MPa
292.1	4.34 \pm 0.11	289.1	1.47 \pm 0.04
292.0	3.57 \pm 0.09	288.9	1.64 \pm 0.04
292.0	3.48 \pm 0.09	288.9	1.42 \pm 0.04
291.3	2.80 \pm 0.07	288.1	1.04 \pm 0.03
291.1	2.54 \pm 0.06	286.8	0.83 \pm 0.02
290.9	2.46 \pm 0.06	286.5	0.95 \pm 0.02
290.5	2.33 \pm 0.06	285.7	0.63 \pm 0.02
290.4	2.20 \pm 0.06	284.4	0.45 \pm 0.01
290.4	1.90 \pm 0.05	282,8	0.28 \pm 0.01
289.8	1.94 \pm 0.05	282.4	0.25 \pm 0.01
289.8	1.84 \pm 0.05	282.2	0.24 \pm 0.01
289.5	1.83 \pm 0.05	281.5	0.16 \pm 0.004
		281.4	0.15 \pm 0.004
		279.7	0.00 \pm 0.004

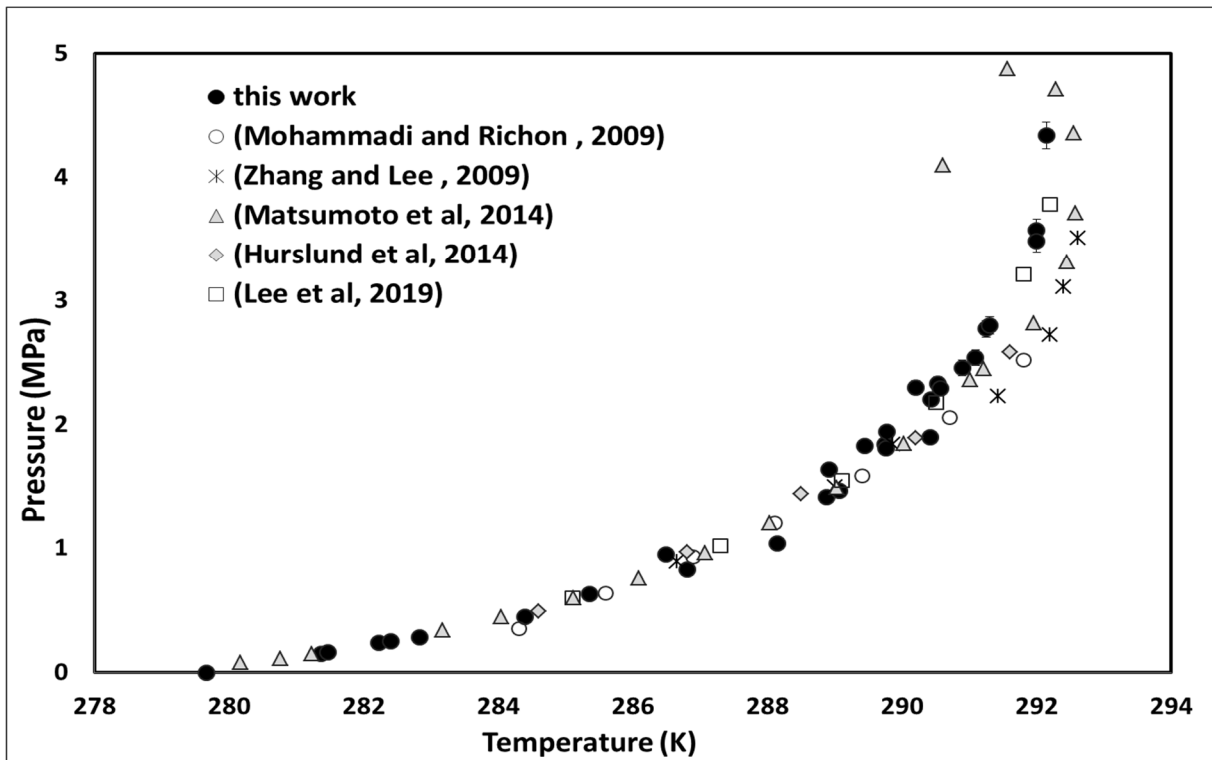


Figure 4: Hydrate + Liquid + Vapor phase equilibria in water + c-C₅H₁₀ + CO₂ system

From Figure 4, it can be seen that our results are generally consistent with literature data. To get an indication of the degree of approximation of our results with all authors, a statistical test called the Mahalanobis test was realized (Table 3). The Mahalanobis distance is an effective multivariate distance metric used to estimate the degree of agreement between two distributions of data sets and to measure the distances between two objects or distributions of data sets (Mahalanobis, 1936). At the same time, several mean values for different variables, here P and T, were measured for each sample. This distance was calculated to rank the equilibrium points obtained in the literature and determine

those closest to our results. The smaller the Mahalanobis distance, the closer are the equilibrium points are to those presented in Table 2. The test was examined in two subgroups. The first subgroup is for points below 289 K and the second subgroup includes all equilibrium points at a temperature above or equal to 289 K.

Table 3: Mahalanobis distance between the equilibrium points of this work and the equilibrium points of each author

	(Herslund <i>et al.</i> , 2014)	(Lee <i>et al.</i> , 2019)	(Matsumoto <i>et al.</i> , 2014)	(Mohammadi and Richon, 2009)	(Zhang and Lee, 2009)
< 289 K	0.596	0.731	0.050	1.141	1.597
≥ 289 K	0.731	0.070	0.856	0.662	1.973

Using this indicator, we can see that our results are in particular agreement with the results of (Lee *et al.*, 2019) at high temperature (≥ 289 K) and pressure and with those of (Matsumoto *et al.*, 2014) at low temperature (< 289 K).

3.2 Dissociation enthalpy

The thermogram can be used to determine the dissociation enthalpy by two methods:

The DSC peak integration. The MicroDSC VII gives a first direct measurement of hydrates dissociation enthalpy. Since the mass of the water sample is precisely known and assuming that water has been converted to hydrates (due to the cycling process), the heat of dissociation per unit mass of water is obtained by integrating the dissociation peak. In the case of incomplete water conversion, it is possible to estimate and subtract the amount of unconverted water by integrating the peak of ice melting that occurs at 273.15 K. This peak corresponds to a heat of dissociation per unit mass of water. This peak corresponds to a heat of fusion of 6 kJ per mole of water.

Clausius-Clapeyron equation. The dissociation enthalpy of gas hydrates can also be calculated using the Clausius-Clapeyron equation from the univariant slope of the phase equilibrium (G.D. Holder *et al.*, 1988) :

$$\frac{d \ln(p)}{d\left(\frac{1}{T}\right)} = \frac{-\Delta H_1}{ZR} \quad (\text{Eq.1})$$

Where p and T are the equilibrium pressure and temperature of the gas hydrate, respectively, ΔH_1 is the dissociation enthalpy of the gas hydrate, per mole of CO₂, Z is the compressibility factor of CO₂, which can be determined by the Benedict Webb Rubin (BWR) equation of state (G.D. Holder *et al.*, 1988; Sandler, 1994), R is the universal gas constant.

Figure 5 plots the equilibrium data in the Clapeyron diagram ($\ln p = f(1/T)$). The enthalpy change, expressed per mole of CO₂, is directly proportional to the slope of the straight line.

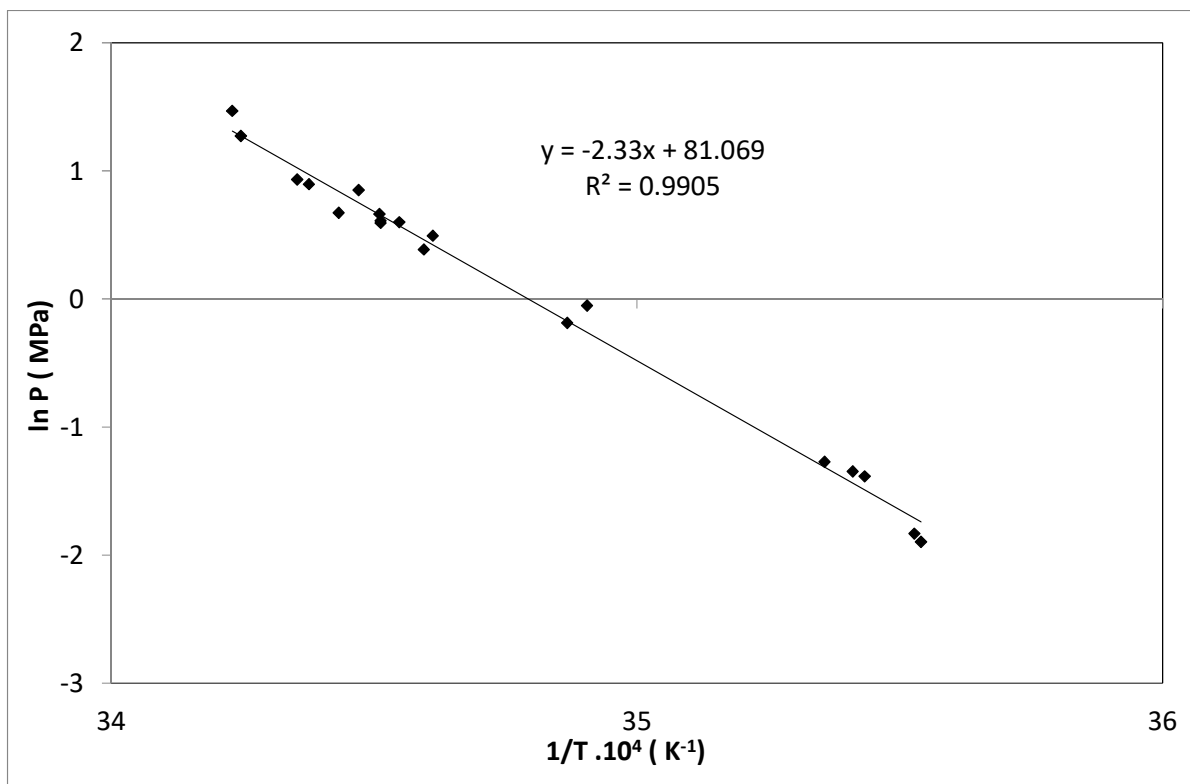


Figure 5: Clapeyron p-T phase diagram

The results are shown in Table 4, where the DSC results are given per mole of water ΔH_2 , while the Clausius-Clapeyron equation results are given per mole of CO₂, ΔH_1 .

It can be seen from Figure 6 that the mixed *c*-C₅H₁₀ + CO₂ hydrates have the highest heat of dissociation over the whole range of pressure compared to other mixed CO₂ containing hydrates. It is about 30 % higher and even higher at low pressure. It can also be found that the enthalpy increases sharply from 406.78 to 466.39 kJ. kg⁻¹ at a pressure equilibrium varying from 0 to 0.5 MPa and then stabilizes around 500 kJ. kg⁻¹ of water at high equilibrium pressure. This value is higher than that of ice and is even greater than the enthalpy of the mixed hydrates TBAB + CO₂. Moreover, the energy of these mixed hydrate can be obtained at lower pressure than concurrent MPCs (less than 1 MPa), which makes their use more efficient.

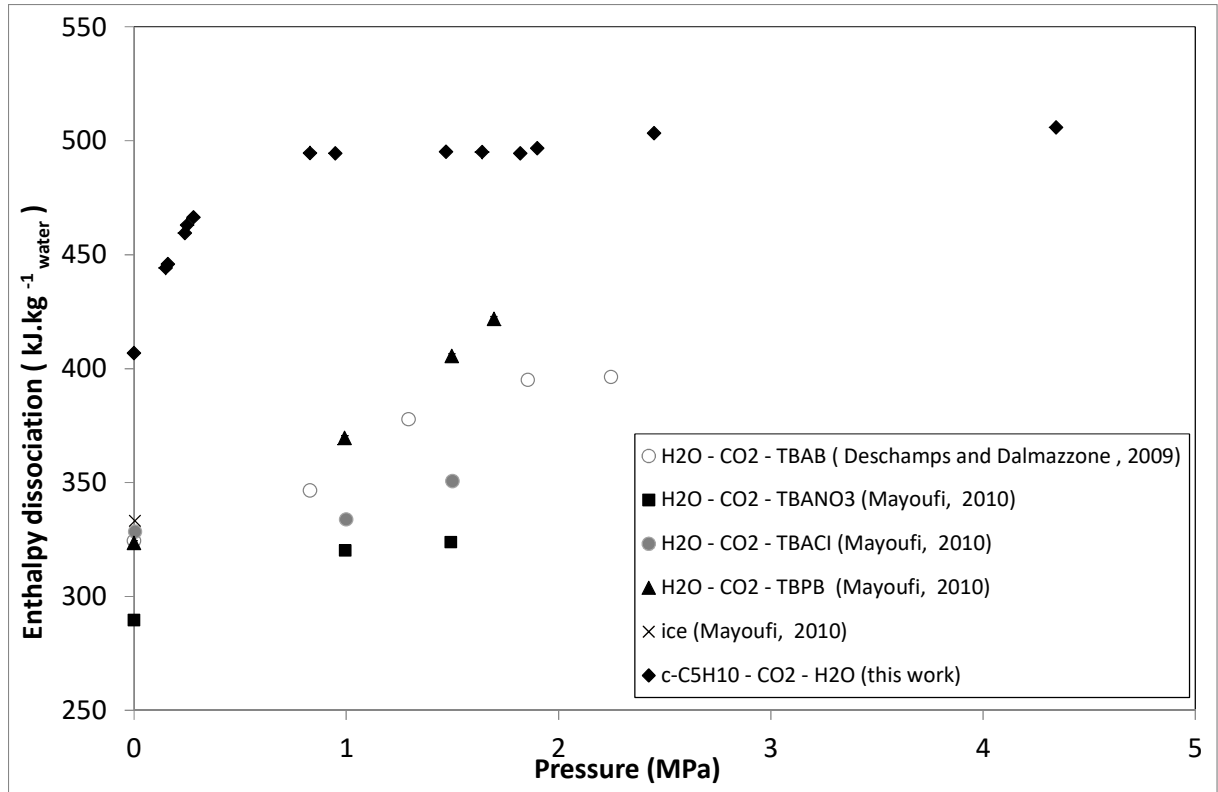
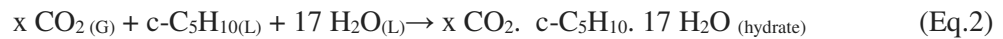


Figure 6: Enthalpy dissociation of mixed hydrates $c\text{-C}_5\text{H}_{10} + \text{CO}_2$ and comparison with data available in the literature

3.3 CO_2 content

Considering that the structure of the mixed $c\text{-C}_5\text{H}_{10} + \text{CO}_2$ hydrates, is a type II cubic clathrate structure (De Hemptinne and Behar, 2000; Sloan Jr *et al.*, 2007), and assuming that the $c\text{-C}_5\text{H}_{10}$ molecules occupy 100 % of the large cavities (Zhang *et al.*, 2004), the formation of the mixed hydrates can be written by the equation (Eq.2):



Based on this equation, the number of moles of hydrate can be obtained from (Eq.3) knowing the number of moles of water converted to hydrate:

$$n_{\text{hydrate}} = 17 \cdot n_{\text{water}} \quad (\text{Eq.3})$$

From the ratio between the hydrate dissociation enthalpy in kilojoules per mole of CO_2 given by the Clausius-Clapeyron equation ΔH_2 , and the experimental DSC values in kilojoules per mole of water ΔH_1 , the ratio x can be calculated (Eq.4).

$$x = \frac{\Delta H_{2/\text{mol H}_2\text{O}}}{\Delta H_{1/\text{mol CO}_2}} \times 17 \quad (\text{Eq.4})$$

Then, the molar number of carbon dioxide n_{CO_2} is calculated from the x values and the molar amount of mixed hydrates n_{hydrate} , using (Eq.5) and presented in Table 4.

$$n_{CO_2} = \frac{n_{hydrate}}{x} \quad (\text{Eq.5})$$

Table 4: Hydrate composition for water + c-C₅H₁₀ + CO₂ system and dissociation enthalpy of mixed c-C₅H₁₀ + CO₂ hydrates at various CO₂ pressures measured by DSC, ΔH₁ and calculated by Clausius-Clapeyron equation, ΔH₂

T /K (±0.2 K)	p /MPa	ΔH ₁ (kJ. mol ⁻¹ CO ₂)	ΔH ₂ (kJ. mol ⁻¹ H ₂ O)	x	n hydrate .10 ³ (mol)	nCO ₂ .10 ³ (mol)
281.4	0.15±0.004	193.38 ± 23	7.99±0.1	0.70±0.1	0.154±0.03	0.219±0.05
281.5	0.16±0.004	193.38 ± 23	8.03±0.2	0.71±0.1	0.154±0.03	0.218±0.05
282.2	0.24±0.01	193.39 ± 24	8.27±0.1	0.73±0.1	0.154±0.03	0.211±0.05
282.4	0.25±0.01	193.39 ± 24	8.33±0.1	0.73±0.1	0.154±0.03	0.210±0.05
282.8	0.28±0.01	193.39 ± 24	8.39±0.1	0.74±0.1	0.154±0.03	0.208±0.05
286.5	0.95±0.02	193.41 ± 24	8.90±0.2	0.78±0.1	0.150±0.03	0.192±0.05
288.9	1.64±0.04	193.42 ± 24	8.91±0.1	0.78±0.1	0.157±0.03	0.200±0.05
289.5	1.82±0.05	193.42 ± 24	8.90±0.1	0.78±0.1	0.150±0.03	0.192±0.05
290.4	1.96±0.05	193.42 ± 24	8.97±0.2	0.79±0.1	0.154±0.03	0.194±0.05
290.9	2.45±0.06	193.42 ± 24	9.06±0.2	0.80±0.1	0.150±0.03	0.189±0.05
292.0	3.57±0.09	193.43 ± 24	8.97±0.1	0.79±0.1	0.157±0.03	0.199±0.05
292.1	4.34±0.11	193.43 ± 24	8.95±0.1	0.79±0.1	0.157±0.03	0.199±0.05

The calculation of n_{CO₂} (Table 4), shows that the amount of CO₂ varies slightly with gas pressure, indicating that there is probably an amount of gas that remains dissolved in the liquid and does not participate in the filling of cavities. This is logical considering that the gas only occupies the small cavities to stabilize the hydrates and that the amount of water and cyclopentane used is the same in all experiments.

Hydration number

Based on knowledge of hydrate structure and gas composition, it is possible to calculate the relative water/guest ratio called the hydration number.

$$nb_h = \frac{n_{H_2O}}{n_{c-C_5H_{10}} + n_{CO_2}} = \frac{17}{1+x} \quad (\text{Eq.6})$$

Mixed c-C₅H₁₀ + CO₂ hydrate have a type II hydrate structure with 16 small cavities and 8 large cavities. Cyclopentane is assumed to occupy all the large cavities, while CO₂ occupies only the small cavities. The values obtained for the hydration number are much higher than the minimum hydration number which is 136 / 24 = 5.67. These values of hydration number are close to the results obtained by Lee et al (Lee *et al.*, 2019) using a different method than the present enthalpy ratio method at a pressure of 3 MPa as shown in Figure 7. No other data seem to be available in the literature to compare our results at other pressures.

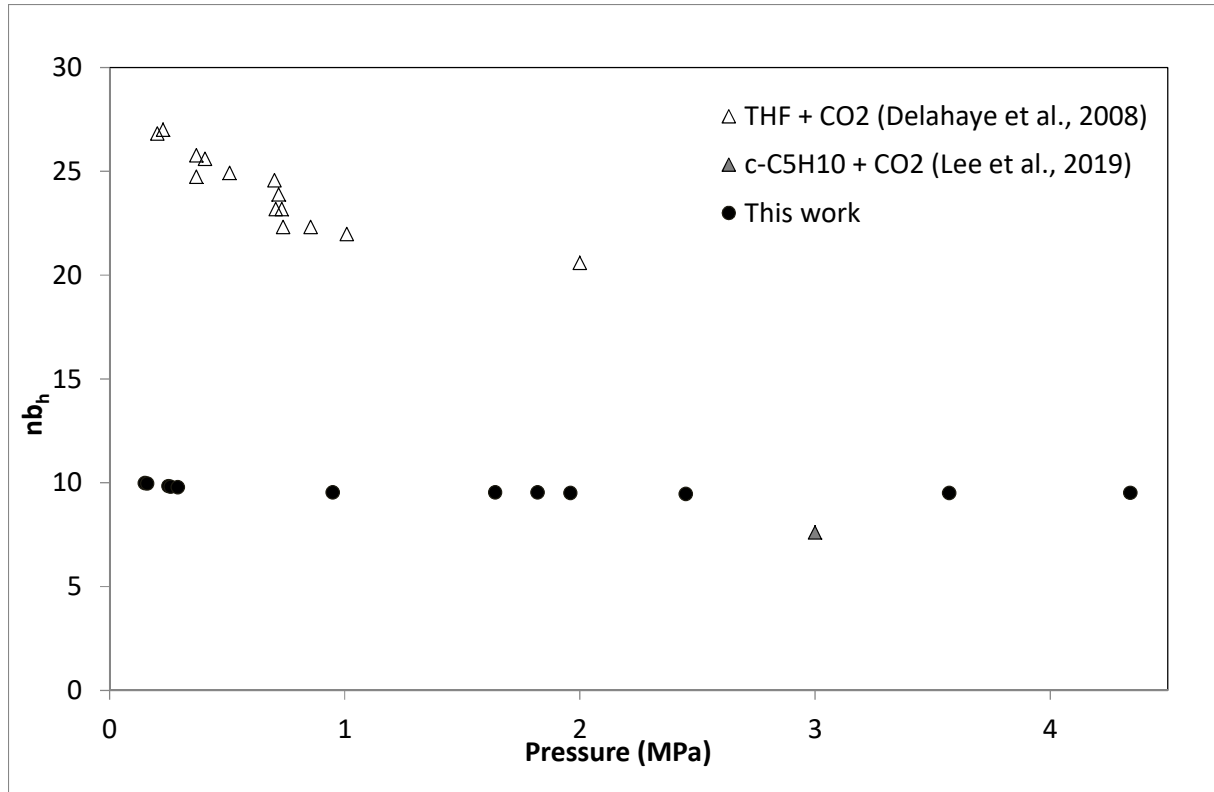


Figure 7: Evolution of the hydration number of CO₂ with pressure into the mixed c-C₅H₁₀ + CO₂ hydrates

As mentioned earlier, the moles number, $n_{hydrate}$ is calculated using the ratio $n_{H_2O}/17$. From this value at 0.25 MPa and using (Eq.2) in the calculation of the molar mass of mixed hydrates, the mass of hydrate formed is estimated as shown in Table 5.

Table 5: Composition of liquid water + liquid hydrocarbon + hydrate + vapor equilibrium

Component	$n_{hydrate}$ (mol)	M (g.mol ⁻¹)	m (mg)	Conversion rate (%)
c-C ₅ H ₁₀ + CO ₂ hydrate	$0.15 \cdot 10^{-3}$	408.23	62.70	100

3.4 Heat capacity of mixed c-C₅H₁₀ + CO₂ hydrates

Heat capacity can be determined from the thermogram analysis. Its determination is rather complicated as it requires a very stable heat flow signal before and after the dissociation peak of the hydrates, which explains the lack of C_p data in the literature. Figure 8 shows the dissociation thermogram of the hydrates at an equilibrium pressure of 0.25 MPa as an example of a stable signal that can be used (Eq.7). At any temperature below 281 K (Figure 8), the sample cell is assumed to contain liquid c-C₅H₁₀, carbon dioxide (gas), and mixed c-C₅H₁₀ + CO₂ hydrates. All the water is assumed to be in the form of hydrates since an excess of c-C₅H₁₀ was used. From these assumptions and from (Eq.8), the determination of the heat capacity of mixed c-C₅H₁₀ + CO₂ hydrate was possible knowing the amount of hydrate formed $n_{hydrate}$, the free gas in the mixture ($n_{CO_2} = n_{CO_2\ init} - n_{CO_2\ consumed}$) (Table 4), and the amount of cyclopentane not consumed during hydrate formation ($n_{c-C_5H_{10}} = n_{c-C_5H_{10}\ init} - 1/17 n_{H_2O\ init}$). In addition, after hydrate dissociation, a quantity of liquid water $n_{i\ H_2O}$, liquid cyclopentane $n_{i\ c-C_5H_{10}}$, and carbon dioxide (gas) remains (Eq.10).

$$C_p = \frac{\dot{q}}{\frac{dT}{dt}} \quad (\text{Eq.7})$$

Where \dot{q} [mW] is the heat flow and $\frac{dT}{dt}$ [K.s⁻¹] is the heating rate of the DSC oven.

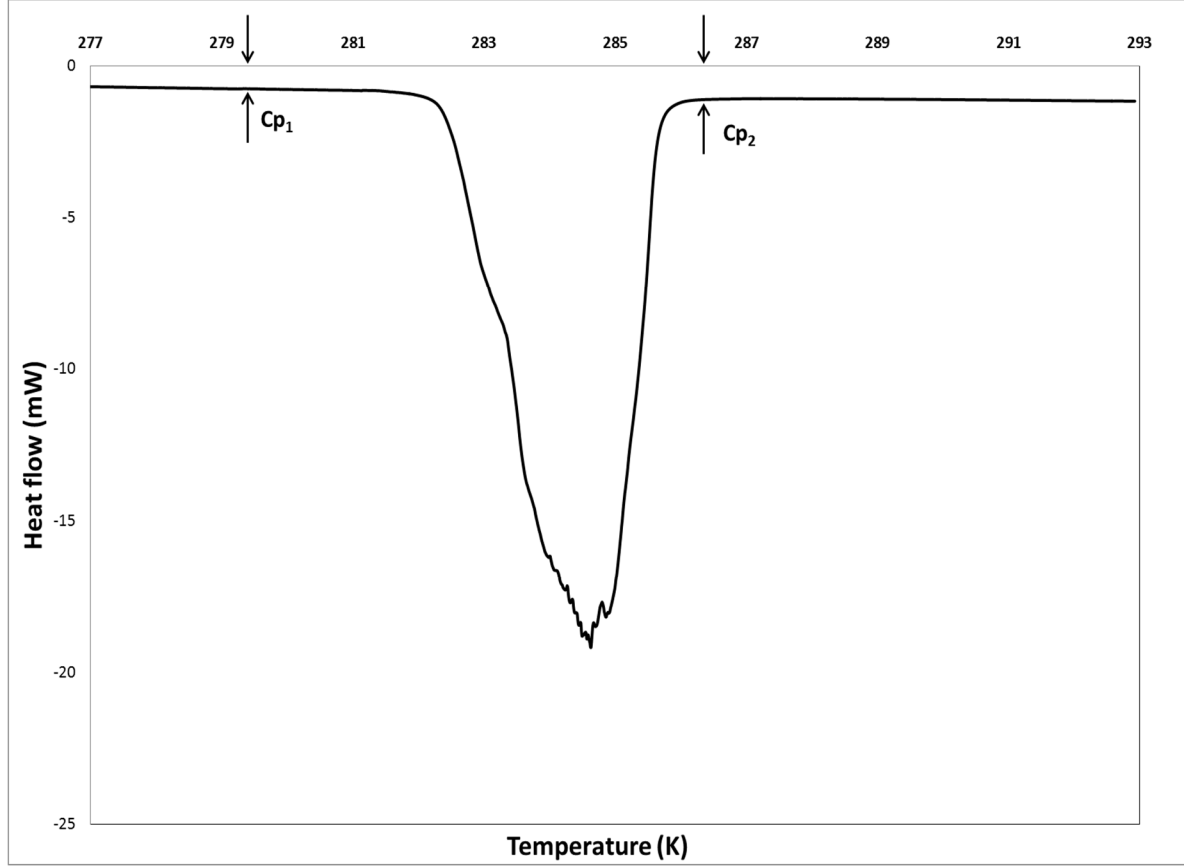


Figure 8: Dissociation thermogram of mixed c-C₅H₁₀ + CO₂hydrates

Table 6: mass heat capacity of mixed c-C₅H₁₀ + CO₂ hydrate before dissociation (C_{p1}), after dissociation (C_{p2})

c-C ₅ H ₁₀ + CO ₂ hydrates	C _{p1}	C _{p2}
C _p (J. K ⁻¹)	0.12 ± 0.01	0.23 ± 0.01
C _p (J. K ⁻¹ . kg ⁻¹)	962.5 ± 71	1862.5 ± 65

The determination of C_{p1} facilitates the calculation of the mixed hydrates heat capacity using (Eq.8)

$$C_{p1} = m_H c_{pH} + m_{c-C_5H_{10}} c_{p_{c-C_5H_{10}}} + m_{CO_2} c_{p_{CO_2}} \quad (\text{Eq.8})$$

$$c_{pH} = \frac{C_{p1} - m_{c-C_5H_{10}} c_{p_{c-C_5H_{10}}} - m_{CO_2} c_{p_{CO_2}}}{m_H} \quad (\text{Eq.9})$$

$$C_{p2} = m_{H_2O} c_{p_{H_2O}} + m'_{c-C_5H_{10}} c_{p_{c-C_5H_{10}}} + m'_{CO_2} c_{p_{CO_2}} \quad (\text{Eq.10})$$

Mixed $c\text{-C}_5\text{H}_{10} + \text{CO}_2$ hydrates form in a closed system that allows the mass of water and cyclopentane in the system to be considered constant after dissociation of $c\text{-C}_5\text{H}_{10} + \text{CO}_2$ hydrates. From this hypothesis, the determination of the composition of different components becomes easier. Thus, C_{pH} at different temperatures can be easily calculated from (Eq.8) using the experimental data of C_{p1} reported in the literature and the heat capacity of different components of mixed hydrates (Table 7) (Table 8)

Table 7: heat capacity formers (Osborne *et al.*, 1972; Yaws, 1996)

Parameter	Cyclopentane	Carbon dioxide	Water
C_p (J. K ⁻¹ . kg ⁻¹)	1740	861	4194

Table 8: heat capacity of hydrate at a range of temperature [277.9 – 282.2] K

T (K) (±0.2 K)	C_{p1} (J. K ⁻¹) (±0.01 J. K ⁻¹)	C_{p1} (J. K ⁻¹ . kg ⁻¹) (±71 J. K ⁻¹ . kg ⁻¹)	C_{pH} (J. K ⁻¹ . kg ⁻¹ _{hydrate}) (±137 J. K ⁻¹ . kg ⁻¹ _{hydrate})	C_{pH} (J. K ⁻¹ . kg ⁻¹ _{water}) (±251 J. K ⁻¹ . kg ⁻¹ _{water})
277.9	0.102	850	1263.8	1685.9
278.4	0.105	875	1311.6	1749.8
278.7	0.108	900	1359.5	1813.6
279.0	0.111	925	1407.3	1877.4
279.6	0.114	950	1455.2	1941.3
279.9	0.117	975	1503.0	2005.1
280.2	0.120	1000	1550.9	2068.9
280.5	0.123	1025	1598.7	2132.6
280.8	0.126	1050	1646.6	2196.6
281.2	0.129	1075	1694.4	2260.4

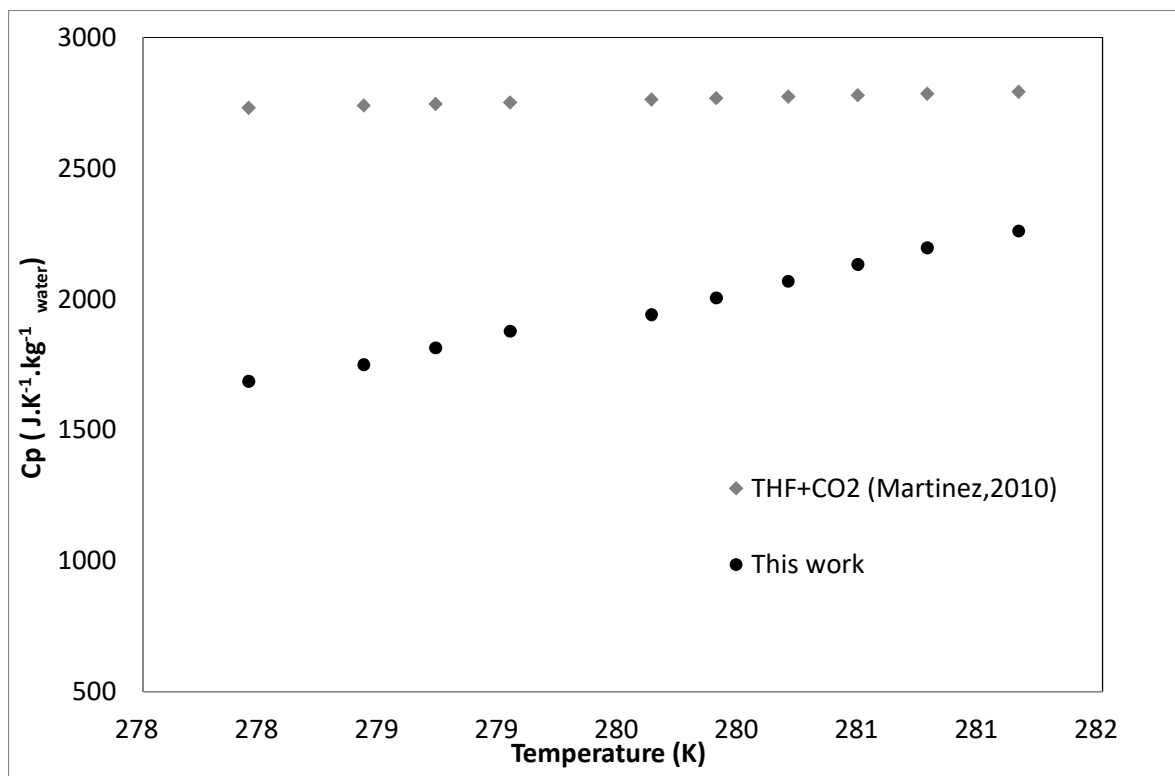


Figure 9: C_p values of mixed $c\text{-C}_5\text{H}_{10} + \text{CO}_2$ hydrates at 0.25 MPa and THF + CO_2 at 0.37 MPa

The evolution of heat capacity with temperature was obtained between 277.9 K and 281.2 K. In Figure 9, the values of C_p of mixed $c\text{-C}_5\text{H}_{10}$ hydrates at equilibrium pressure 0.25 MPa in $\text{J.K}^{-1}.\text{kg}^{-1}_{\text{water}}$ are shown to be compared with (Martinez Valentin-Gamazo, 2009) results (the THF + CO_2 hydrates heat capacity correlation obtained from experimental data at 0.37 MPa). As can be seen in Figure 9, the $C_{p,H}$ values increase with increasing temperature; this variation is much more significant for mixed $c\text{-C}_5\text{H}_{10} + \text{CO}_2$ hydrates than for THF + CO_2 hydrates.

Conclusion

The aim of the present work was to determine the formation conditions and thermophysical properties of mixed $c\text{-C}_5\text{H}_{10} + \text{CO}_2$ hydrates, in view of their possible use as cold storage material and secondary refrigerants. The four phase ($L_W\text{-}L_{CP}\text{-}H\text{-}V$) equilibrium conditions of the hydrates formed in the $c\text{-C}_5\text{H}_{10} + \text{CO}_2 + \text{water}$ system were studied by the DSC method in the presence of an excess of cyclopentane. The equilibrium results presented in this work cover a wide pressure range (from very low to high pressures). It was found that the formation conditions of mixed hydrates in the presence of cyclopentane as promoter are weaker than those of simple CO_2 hydrates.

A multi-cycle DSC method was implemented to measure dissociation enthalpy of the mixed $c\text{-C}_5\text{H}_{10} + \text{CO}_2$ hydrates in a pressure range that varies between 0 and 4.3 MPa. The variation of enthalpy with pressure showed two distinct trends: In a first pressure interval from 0 to 0.5 MPa, the enthalpy increases with pressure from 406.78 to 466.39 $\text{kJ.kg}^{-1}_{\text{water}}$ ($462.5 \pm 1.5 \text{kJ.kg}^{-1}_{\text{water}}$ at the equilibrium point (282.4 K, 0.25 MPa)). In a second interval, for high pressure, the enthalpy remains almost constant around a value of 500 $\text{kJ.kg}^{-1}_{\text{water}}$.

The DSC curves were also used to determine the average mass heat capacity of the mixed hydrates, $1479 \pm 137 \text{J.K}^{-1}.\text{kg}^{-1}$ of hydrates at 0.25 MPa in a temperature range between 277.9 K and 281.2 K. No data were found in the literature for the heat capacity of the mixed $c\text{-C}_5\text{H}_{10} + \text{CO}_2$ hydrates at any thermodynamic equilibrium conditions.

The hydrate mass and molar mass were estimated assuming that the total amount of water was consumed during hydrate formation. Therefore, the mixture of water + *c*-C₅H₁₀ + CO₂ allowed the formation of mixed *c*-C₅H₁₀ + CO₂ hydrates with a conversion rate of 100 % of water. The equilibrium and enthalpy results were also used to estimate the composition of the mixed hydrates formed at different CO₂ pressures.

The experimental results presented in this work could be used to validate or develop a thermodynamic model for mixed *c*-C₅H₁₀ + CO₂ hydrates and to guide further work on hydrate slurries applied in secondary refrigeration and cold storage.

Acknowledgements

This work was supported by the French National Research Agency under the program MUSCOFI (ANR-18-CE0-0028), and undertaken in the frame of the US Partnership for International Research and Education program (National Science Foundation Award Number 1743794) and of the French Research Consortium “GDR-2026 Hydrates de gaz”.

References

- Carroll, J., 2014. Natural Gas Hydrates A Guide for Engineers, Third Edit.
- Clain, P., Ndoye, F.T., Delahaye, A., Fournaison, L., Lin, W., Dalmazzone, D., 2015. Particle size distribution of TBPB hydrates by focused beam reflectance measurement (FBRM) for secondary refrigeration application. *International Journal of Refrigeration* 50, 19–31. <https://doi.org/10.1016/j.ijrefrig.2014.10.016>
- De Hemptinne, J., Behar, E., 2000. Thermodynamic properties of acid gas containing systems: Literature review. *Oil Gas Sci. Technol.* 55, 617–637.
- G.D. Holder, S.P. Zetts, N. Pradhan, 1988. Phase Behavior in Systems Containing Clathrate Hydrates: A Review. *Reviews in Chemical Engineering* 5, 1–70. <https://doi.org/10.1515/REVCE.1988.5.1-4.1>
- Herslund, P.J., Daraboina, N., Thomsen, K., Abildskov, J., von Solms, N., 2014. Measuring and modelling of the combined thermodynamic promoting effect of tetrahydrofuran and cyclopentane on carbon dioxide hydrates. *Fluid Phase Equilibria* 381, 20–27. <https://doi.org/10.1016/j.fluid.2014.08.015>
- Jeffrey, G.A., 1984. Hydrate inclusion compounds. *Journal of inclusion phenomena* 1, 211–222. <https://doi.org/10.1007/BF00656757>
- Kang, S.-P., Lee, H., 2000. Recovery of CO₂ from flue gas using gas hydrate: thermodynamic verification through phase equilibrium measurements. *Environmental science & technology* 34, 4397–4400.
- Lee, J., Kim, K.-S., Seo, Y., 2019. Thermodynamic, structural, and kinetic studies of cyclopentane + CO₂ hydrates: Applications for desalination and CO₂ capture. *Chemical Engineering Journal* 375, 121974. <https://doi.org/10.1016/j.cej.2019.121974>
- Mahalanobis, P.C., 1936. On the Generalised Distance in Statistics. *On the Generalized Distance in Statistics* 49–55.
- Marinhas, S., Delahaye, A., Fournaison, L., Dalmazzone, D., Fürst, W., Petitet, J.-P., 2006. Modelling of the available latent heat of a CO₂ hydrate slurry in an experimental loop applied to secondary refrigeration. *Chemical Engineering and Processing: Process Intensification* 45, 184–192. <https://doi.org/10.1016/j.cep.2005.08.002>
- Martinez Valentin-Gamazo, M. del C., 2009. Étude des coulis d'hydrates de CO₂ en présence d'additifs pour la réfrigération secondaire (PhD Thesis).
- Matsumoto, Y., Makino, T., Sugahara, T., Ohgaki, K., 2014. Phase equilibrium relations for binary mixed hydrate systems composed of carbon dioxide and cyclopentane derivatives. *Fluid Phase Equilibria* 362, 379–382. <https://doi.org/10.1016/j.fluid.2013.10.057>
- Mayoufi, N., Dalmazzone, D., Fürst, W., Delahaye, A., Fournaison, L., 2010. CO₂ enclathration in hydrates of peralkyl-(Ammonium/Phosphonium) salts: Stability conditions and dissociation enthalpies. *Journal of Chemical and Engineering Data* 55, 1271–1275. <https://doi.org/10.1021/je9006212>
- Mohammadi, A.H., Richon, D., 2009. Phase equilibria of clathrate hydrates of methyl cyclopentane, methyl cyclohexane, cyclopentane or cyclohexane+carbon dioxide. *Chemical Engineering Science* 64, 5319–5322. <https://doi.org/10.1016/j.ces.2009.09.048>
- Mondal, M.K., Balsora, H.K., Varshney, P., 2012. Progress and trends in CO₂ capture/separation technologies: A review. *Energy* 46, 431–441. <https://doi.org/10.1016/j.energy.2012.08.006>
- Oignet, J., Hoang, H.M., Osswald, V., Delahaye, A., Fournaison, L., Haberschill, P., 2017. Experimental study of convective heat transfer coefficients of CO₂ hydrate slurries in

- a secondary refrigeration loop. *Applied Thermal Engineering* 118, 630–637.
<https://doi.org/10.1016/j.applthermaleng.2017.02.117>
- Osborne, J., Stimson, M., Ginnings, S., 1972. *Handbook of Chemistry and Physics*. Cleveland.
- Oyama, H., Shimada, W., Ebinuma, T., Kamata, Y., Takeya, S., Uchida, T., Nagao, J., Narita, H., 2005. Phase diagram, latent heat, and specific heat of TBAB semiclathrate hydrate crystals. *Fluid Phase Equilibria* 234, 131–135.
<https://doi.org/10.1016/j.fluid.2005.06.005>
- Sakamoto, H., Sato, K., Shiraiwa, K., Takeya, S., Nakajima, M., Ohmura, R., 2011. Synthesis, characterization and thermal-property measurements of ionic semi-clathrate hydrates formed with tetrabutylphosphonium chloride and tetrabutylammonium acrylate. *RSC Advances* 1, 315–322. <https://doi.org/10.1039/c1ra00108f>
- Sandler, S.I., 1994. Equations of state for phase equilibrium computations, in: *Supercritical Fluids*. Springer, pp. 147–175.
- Sloan Jr, E.D., Koh, C.A., Koh, C., 2007. *Clathrate hydrates of natural gases*. CRC press.
- Taheri, Z., Shabani, M.R., Nazari, K., Mehdizadeh, A., 2014. Natural gas transportation and storage by hydrate technology: Iran case study. *Journal of Natural Gas Science and Engineering* 21, 846–849. <https://doi.org/10.1016/j.jngse.2014.09.026>
- Wenji, S., Rui, X., Chong, H., Shihui, H., Kaijun, D., Ziping, F., 2009. Experimental investigation on TBAB clathrate hydrate slurry flows in a horizontal tube: Forced convective heat transfer behaviors. *International Journal of Refrigeration* 32, 1801–1807. <https://doi.org/10.1016/j.ijrefrig.2009.04.008>
- Yaws, C.L., 1996. *Handbook of Thermodynamic Diagrams : Organic compounds C5 to C7*, Gulf Pub. Co. ed.
- Zhang, J.S., Lee, J.W., 2009. Equilibrium of Hydrogen + Cyclopentane and Carbon Dioxide + Cyclopentane Binary Hydrates. *J. Chem. Eng. Data* 54, 659–661.
<https://doi.org/10.1021/je800219k>
- Zhang, Y., Debenedetti, P.G., Prud'homme, R.K., Pethica, B.A., 2004. Differential scanning calorimetry studies of clathrate hydrate formation. *The Journal of Physical Chemistry B* 108, 16717–16722.